Traffic 2007; **8:** 61–76
Blackwell Munksgaard

doi: 10.1111/j.1600-0854.2006.00512.x

Dynamic Interaction of HIV-1 Nef with the Clathrin-Mediated Endocytic Pathway at the Plasma Membrane

Anne Burtey[1,2,3,4], Joshua Z. Rappoport[5], Jérôme Bouchet[1,2,3,4], Stéphane Basmaciogullari[1,2,3,4], John Guatelli[6], Sanford M. Simon[5], Serge Benichou[1,2,3,4]*, and Alexandre Benmerah[1,2,3,4]*

[1]Institut Cochin, Département Maladies Infectieuses, Paris F-75014, France
[2]Inserm, U567, Paris F-75014, France
[3]CNRS, UMR 8104, Paris F-75014, France
[4]Université Paris 5, Faculté de Médecine René Descartes, Paris F-75014, France
[5]The Laboratory of Cellular Biophysics, The Rockefeller University, 1230 York Avenue, Box 304, New York, NY 10021, USA
[6]Department of Medicine University of California, San Diego, 9500 Gilman Drive, La Jolla, CA 92093, USA
**Corresponding author: Alexandre Benmerah or Serge Benichou, benmerah@cochin.inserm.fr or benichou@cochin.inserm.fr*

The HIV-1 Nef protein perturbs the trafficking of membrane proteins such as CD4 by interacting with clathrin–adaptor complexes. We previously reported that Nef alters early/recycling endosomes, but its role at the plasma membrane is poorly documented. Here, we used total internal reflection fluorescence microscopy, which restricts the analysis to a ~100 nm region of the adherent surface of the cells, to focus on the dynamic of Nef at the plasma membrane relative to that of clathrin. Nef colocalized both with clathrin spots (CS) that remained static at the cell surface, corresponding to clathrin-coated pits (CCPs), and with ~50% of CS that disappeared from the cell surface, corresponding to forming clathrin-coated vesicles (CCVs). The colocalization of Nef with clathrin required the di-leucine motif essential for Nef binding to AP complexes and was independent of CD4 expression. Furthermore, analysis of Nef mutants showed that the capacity of Nef to induce internalization and downregulation of CD4 in T lymphocytes correlated with its localization into CCPs. In conclusion, this analysis shows that Nef is recruited into CCPs and into forming CCVs at the plasma membrane, in agreement with a model in which Nef uses the clathrin-mediated endocytic pathway to induce internalization of some membrane proteins from the surface of HIV-1-infected T cells.

Key words: clathrin, endocytosis, HIV-1, live cell imaging, Nef

Received 21 March 2006; revised and accepted for publication 19 October 2006; published online 21 November 2006

The *nef* gene product of HIV-1 is a 27-kDa protein that associates with cell membranes through N-terminal myristoylation. Like other HIV-1 accessory proteins, Nef is essential for maximal viral replication *in vivo* and markedly contributes to the pathogenesis of AIDS. *In vitro*, Nef modulates T-cell activation and alters the intracellular distribution of a number of cellular proteins. These effects facilitate viral replication, in part by enhancing the infectivity of virions [reviewed by Fackler and Baur and Wei et al. (1,2)].

The positive influence of Nef on viral replication and infectivity is a multifactorial process but relates, at least in part, to the disturbance of the trafficking of membrane proteins within the endocytic pathway. Nef both misdirects CD4, the primary receptor for HIV, from the *trans* Golgi network (TGN) to endosomes and stimulates its internalization from the cell surface, resulting in an accumulation of CD4 in the early/sorting endosomal compartment. CD4 is ultimately targeted to lysosomes where it is degraded. Together, these Nef-mediated effects drastically reduce the level of cell surface-associated CD4 molecules at steady state, a process collectively referred as 'CD4 downregulation' (3–6).

These observations led to the hypothesis that Nef functions as a specific connector between the cytoplasmic domain of CD4 and the endosomal and TGN-associated protein sorting machineries [reviewed by Piguet et al. (7)]. However, it was subsequently reported that Nef also affected the steady-state distribution and endocytosis of the class I major histocompatibility complex (MHC) molecules (5). More recently, the list of cellular membrane-associated proteins whose intracellular trafficking is altered by Nef has expanded to include mature and immature class II MHC, the costimulatory CD28 molecules, the lectin DC-SIGN (dendritic cell-specific ICAM-grabbing non integrin) expressed on dendritic cells, the CCR5 and CXCR4 chemokine coreceptors and also the transferrin receptor (TfR) (8–13). This increasing number of proteins whose trafficking is altered during infection suggests that Nef is unlikely to be a specific adaptor but rather exerts a more general effect on the endocytic system.

The mechanisms responsible for these widespread Nef-mediated effects are not fully understood but are likely related to the ability of Nef to interact with essential components of the machineries involved in the budding of transport vesicles and protein sorting. Indeed, Nef directly interacts with the clathrin–adaptor protein (AP)

complexes that govern clathrin polymerization on specific membranes (TGN, endosomes or plasma membrane) and cargo selection for vesicular transport (4,5,14,15). Nef also interacts directly with the catalytic subunit of the vacuolar adenosine triphosphatase required for acidification of endosomes, and with the PACS-1 protein (phosphofurin acidic cluster sorting protein-1) involved in TGN localization of membrane proteins containing acidic cluster motifs (16–18).

Four distinct types of AP complexes (AP-1 to AP-4) have been characterized and consist of heterotetramers composed of two large subunits (adaptins: α, δ, γ or ϵ, and β1-4), one medium chain (μ1–4) and one small subunit (σ1–4). With the exception of AP-2, the association of AP complexes with membranes is regulated by ADP ribosylation factor 1 (ARF1). While AP-1, AP-3 and AP-4 mediate transport between the TGN and the endosomes or lysosomes, AP-2 is specifically localized to plasma membrane where it plays a central role in both the assembly and the function of clathrin-coated pits (CCPs) (19). The sorting function of AP complexes is related to the recognition of specific signals present in the cytoplasmic domain of transmembrane trafficking proteins. These signals are based on tyrosine or leucine residues that conform to the sequences YXX Φ or E/DXXXLΦ [where Φ is a bulky hydrophobic residue; reviewed by Bonifacino and Traub (20)].

Interestingly, HIV-1 Nef contains a canonical leucine-based AP-binding motif located within an unstructured loop found in the C-terminal part of the protein. The presence of this di-leucine motif is critical for the Nef effects on CD4 and some other receptors but not for its effects on MHC-I molecules (14,15,17,18,21–24). It is also required for the maximal infectivity of HIV-1 virions (13,25,26), indicating that the positive influence of Nef on viral infectivity is related, at least in part, to its general impact on the endosomal system. Although the specific contributions and the dynamics of the association of Nef with the individual AP complexes are still unclear, previous *in vitro* studies suggested that the HIV-1 Nef protein preferentially interacts with AP-1 and AP-3 complexes (24,26,27). In living cells, Nef recruits and stabilizes the association of AP-1 and AP-3 on endosomal membranes by an ARF1-independent mechanism (27), resulting in morphological and functional alterations of the early/sorting endosomal compartments (13,28–30). In contrast, the specific role of Nef at the plasma membrane and how this myristoylated protein reaches early endosomes are poorly documented. Paradoxically, although HIV-1 Nef interacts at best weakly with the intact AP-2 complex (5,23,24,26,31), its ability to accelerate the rate of internalization of CD4 from the cell surface suggests a role for clathrin-mediated endocytosis in Nef action (32).

To clarify the action of Nef at the cell surface in relation to the clathrin-dependent endocytic pathway, we investigated the dynamic behavior of Nef at the plasma membrane of living cells using total internal reflection fluorescence microscopy (TIR-FM). This technique restricts the morphologic analysis of the samples to the adherent surface of the cells and has been recently extensively used to study the dynamics of clathrin and clathrin-associated proteins (33,34). Here, TIR-FM revealed the specific localization of Nef in CCPs and in forming clathrin-coated vesicles (CCVs) at the plasma membrane and was further used to characterize the mechanisms responsible for this localization using Nef mutants and CD4-expressing cell lines. Finally, the results obtained by TIR-FM were challenged by testing the effect of the same Nef variants on CD4 endocytosis in T lymphocytes.

Results

Epifluorescence microscopy does not allow analysis of Nef at the plasma membrane

To follow the dynamic behavior of Nef at the plasma membrane in living cells, we used a green fluorescent protein (GFP)-tagged construct for expression of the HIV-1 NL4-3 Nef protein fused to the N-terminus of GFP. This Nef–GFP fusion was previously shown to recapitulate the activity of wild-type Nef in a variety of assays including the downregulation of cell surface receptors, such as CD4 (13,23,35). The distribution of Nef–GFP was compared with that of clathrin by coexpression of a DsRed-tagged clathrin light chain chimera used previously to characterize the dynamics of clathrin at the plasma membrane (36,37).

The subcellular distribution of both Nef–GFP and DsRed-clathrin was first assessed by epifluorescence on either fixed (Figure 1) or live (not shown) transiently transfected HeLa cells. As previously shown (13), Nef–GFP was concentrated in intracellular perinuclear structures (Figure 1A), which corresponded to enlarged early/sorting endosomes. This perinuclear distribution of Nef–GFP also overlapped with DsRed-clathrin (Figure 1A,B), a result in agreement with the previously described colocalization of Nef with both the AP-1 and the AP-3 clathrin–adaptor complexes (13,29). When the focus was shifted to the adherent surface of transfected cells to observe plasma membrane-associated DsRed-clathrin in CCPs (CCPs; Figure 1D), Nef–GFP fluorescence was in general diffuse (Figure 1C). Closer inspection showed that Nef–GFP could also be found in spots brighter than the local background, and these spots colocalized with DsRed-clathrin (Figure 1C,D, enlarged pictures). These data indicated a potential localization of Nef–GFP in CCPs. However, the spots observed for Nef–GFP were barely distinguishable from background fluorescence; this precluded the use of epifluorescence to follow the dynamic of Nef at the plasma membrane.

TIR-FM reveals the localization of HIV-1 Nef in clathrin-coated structures at the plasma membrane

Epifluorescence microscopy leads to the illumination of the whole sample and excitation of fluorophores and

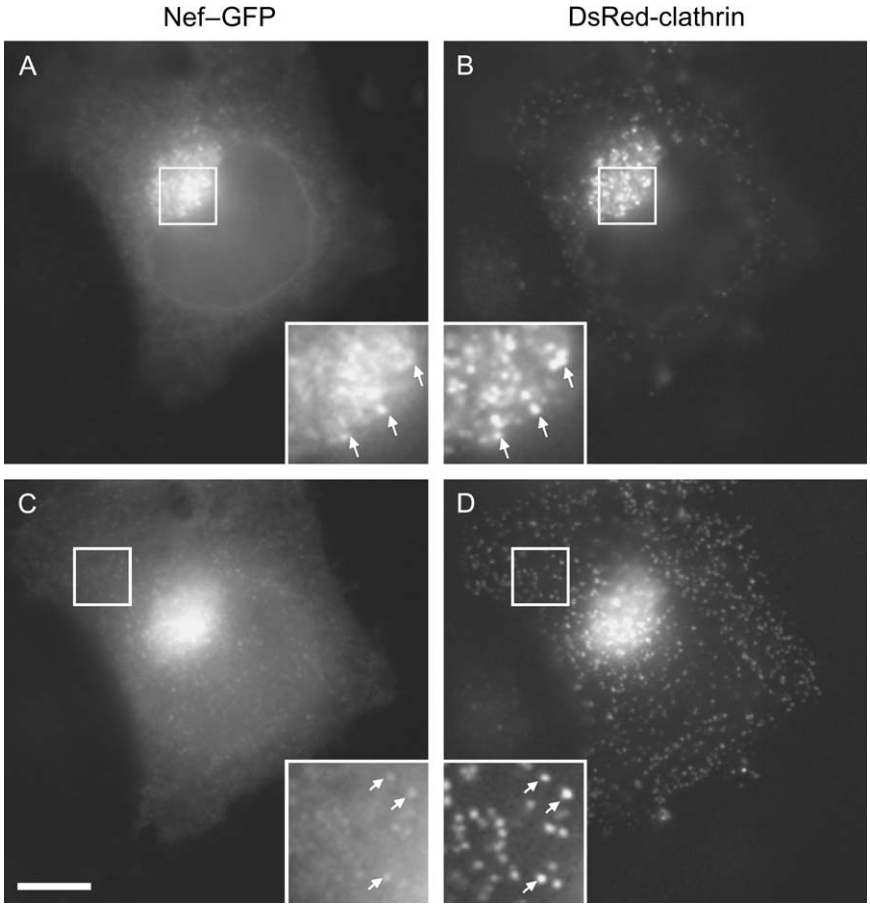

Figure 1: Distribution of Nef–GFP observed by epifluorescence. HeLa cells were transfected with plasmids encoding wild-type HIV-1 Nef fused to GFP (Nef–GFP, A and C) and clathrin light chain fused to DsRed (B and D). Cells were then fixed and observed by epifluorescence. The focus was made on a medial region (A and B) and on the adherent surface (C and D) of the same cells. Insets show higher magnification (×2.5) of representative areas. Arrows stress colocalization of both markers. Scale bar, 10 μm.

fluorescent proteins out of the focal plane. Therefore, observation of Nef at the plasma membrane is masked by the strong fluorescence emitted in the perinuclear region (Figure 1A,C). To make possible the detection of Nef in plasma membrane-associated CCPs, we used TIR-FM. TIR-FM produces an evanescent field at the interface between the glass and the cell culture media that decays to 1/e in approximately 100 nm in our experimental system. Thus, the excitation of fluorophores decreases exponentially as a function of distance from the glass and therefore allows excitation of fluorophores found in a region encompassing the extracellular milieu, the plasma membrane and a thin layer of cytoplasm. This technique has been recently used extensively to follow the dynamics of plasma membrane-associated events including the assembly and budding of CCP/CCV [reviewed by Rappoport et al. and Perrais and Merrifield (33,34)].

Transiently transfected live HeLa cells expressing both Nef–GFP and DsRed-clathrin were then observed by TIR-FM. The results shown in Figure 2 clearly exemplified the advantage of this technique. Because only the plasma membrane-associated fluorescent proteins were excited by the evanescent wave, the strong intracellular staining observed by epifluorescence for both Nef and clathrin was completely lost. In these conditions, Nef–GFP still showed a diffuse staining at the plasma membrane but was also clearly concentrated in punctate structures that colocalized with DsRed-clathrin (Figure 2A,B, arrows). The level of colocalization of Nef with clathrin was quantified by measuring both GFP and DsRed fluorescence intensity in ~1000 spots from seven different cells. Fluorescence from DsRed was used to identify clathrin spots (CS). Each CS was circled, and the resulting regions were transferred to the GFP images to quantify the intensity of Nef-associated fluorescence within each CS normalized to local background as indicated in *Materials and Methods*. An individual CS was considered to also contain Nef when GFP-associated normalized fluorescence was at least 10% above local background (greater than 1.09), a limit value generally in agreement with what can be detected as a spot by direct observation (data not shown). Using this method, ~60% of total CS were found to also contain Nef at level above local background (Figure 2C). With the same method, we conversely quantified the intensity of clathrin-associated fluorescence in Nef–GFP-positive spots, and almost all (~93%) of these Nef spots contained clathrin. These results indicated that a majority of but not all CS contained Nef and that most if not all Nef spots correspond to CS. Given that the large majority of CS (>90%) observed at the plasma membrane by TIR-FM correspond to AP-2-containing CCP and/or forming CCV [reviewed by Rappoport et al. and

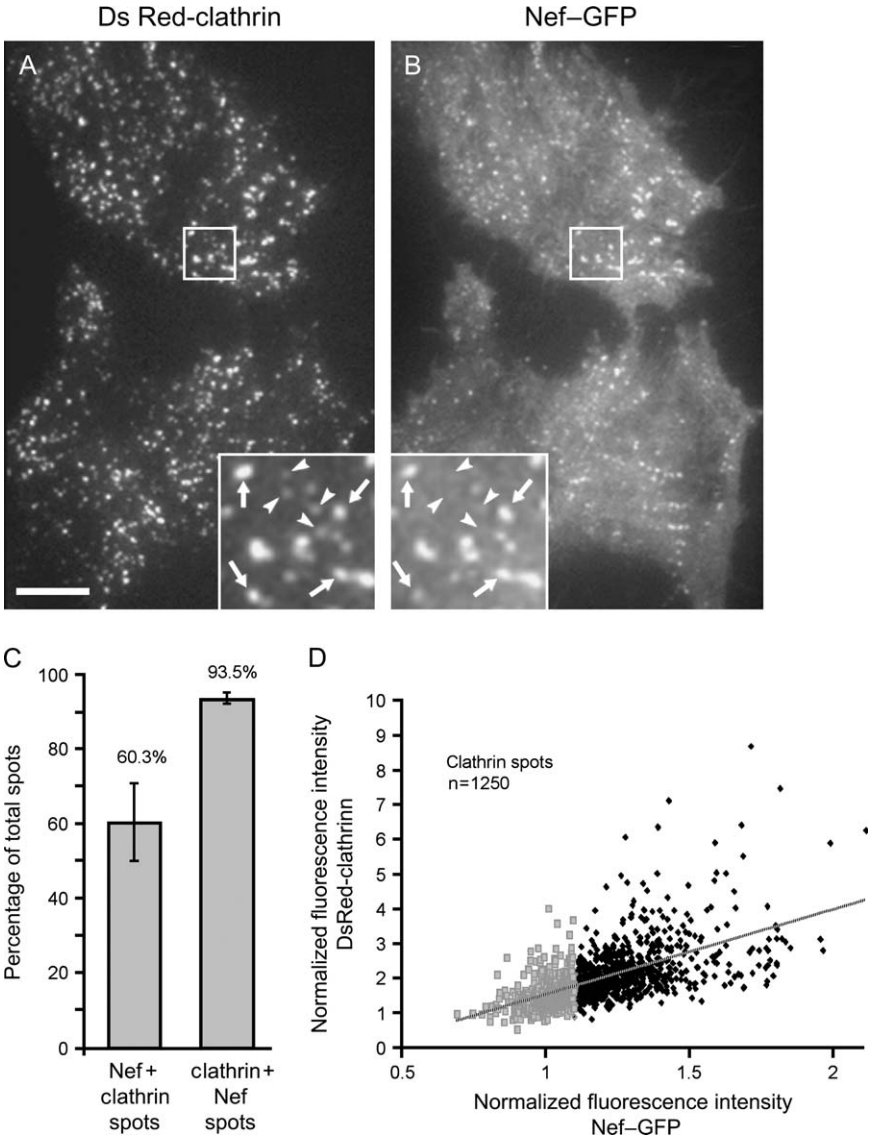

Figure 2: TIR-FM reveals the colocalization of Nef with clathrin at the plasma membrane. Live HeLa cells expressing DsRed-cathrin (A) and Nef–GFP (B) were imaged by TIR-FM. Insets show higher magnification (×3) of a representative area. Arrows stress colocalizing spots and arrowheads CS in which Nef is not concentrated. Scale bar, 10 μm. C) Colocalization of Nef–GFP within CS was quantified using MetaMorph software as indicated in *Materials and Methods*. Briefly, CS (>1000 spots, seven cells) were circled, and GFP- and DsRed-associated fluorescence intensities were collected and normalized to the local background. The presence of Nef within CS was then quantified by selecting Nef spots with a normalized fluorescence intensity above 1.1, a value corresponding to a detectable increased fluorescence relative to background, a 'spot', by direct observation (data not shown). Conversely, the presence of clathrin within Nef spots was similarly quantified. D) Spots analyzed in (C) were plotted in function of their normalized fluorescence for both clathrin and Nef. Spots with a normalized fluorescence below 1.1 appear in gray.

Perrais and Merrifield (33,34)], these results suggest that Nef accumulates in CCP/CCV at steady state.

The quantification presented above indicated that Nef is effectively concentrated in around 60% of total plasma membrane-associated CS. The lack of apparent concentration of Nef in the remaining 40% CS might be due to a detection problem linked to the high fluorescence background at the plasma membrane observed for Nef. Indeed, the fluorescence intensity of clathrin in CS is highly heterogeneous with very bright to dim CS (Figure 2A,C), but because of the very low background fluorescence, even the dimmer CS could be clearly identified by direct observation (Figure 2A, arrowheads). Interestingly, Nef was not detected in those dimmer CS (Figure 2B, arrowheads), suggesting that the 40% of Nef-negative CS could correspond to the dimmer CS population. To test this hypothesis, spots were plotted as a function of their respective normalized Nef and clathrin fluorescence. As shown in Figure 2, normalized Nef fluorescence intensity was proportional to that of clathrin as indicated by the linear distribution of the spots. In addition and as expected, when spots with normalized Nef fluorescence intensity below 1.1 were selected (gray), almost all of them corresponded to dimmer CS. This analysis suggested that the absence of Nef in 40% of the plasma membrane-associated CS is likely due to an inability to detect Nef in the dimmer CS population.

Altogether, the results reported in Figure 2 show that Nef is concentrated within the majority of the CS observable at the plasma membrane.

Nef is found in both static and disappearing CS at the plasma membrane

Clathrin spots at the plasma membrane can be categorized into three different populations during a 1-min observation: 80% remain static, 15% disappear from the surface and

5% move laterally. The static CS were characterized as AP-2-containing CCPs, the disappearing CS as forming CCVs that move deeper into the cells and leave the evanescent field and the laterally moving CS colocalize with microtubules. It remains to be resolved if the laterally moving CS are on the plasma membrane or represent internal endosomes [reviewed by Rappoport et al. and Perrais and Merrifield (33,34)].

The distribution of Nef in each CS population was evaluated by TIR-FM in live HeLa cells coexpressing Nef–GFP and DsRed-clathrin. Clathrin spots from each category were identified, and the presence of Nef–GFP in these CS was then analyzed. As illustrated in Figures 3 and 4, Nef–GFP was found in the three types of clathrin-positive structures: static, disappearing and laterally mobile. A region of the plasma membrane containing a disappearing CS close to a static CS is shown in Figure 3C and in Video S1. The upper arrowed spot containing both clathrin and Nef at the beginning progressively disappeared from the evanescent field, while the neighboring one remained static. Quantification of fluorescence intensity over time along a line drawn between the two spots on Figure 3C showed that the Nef- and clathrin-associated fluorescence intensities decreased with the same kinetics in the upper disappearing CS, whereas the respective intensities remained stable in the neighboring static spot (Figure 3D). An example of a laterally mobile CS was identified from the clathrin frames shown in Figure 3E, which also contained Nef–GFP (Figure 3G, arrow, and Video S2).

The dynamic behavior of Nef was quantified by analyzing 40 spots from each CS category from at least five different cells and expressed as the percentage of CS containing Nef–GFP (Figure 3H). Nef was not only detected in the large majority of static CS (91.5%), in approximately half of the disappearing CS (50.6%), but also in a minority of laterally mobile CS (22.1%). Altogether, these results indicated that HIV-1 Nef is present in CCPs (static spots) and forming CCVs (disappearing spots) because it disappeared from the evanescent field together with some CS.

The leucine-based motif of Nef is required for targeting into CCP

HIV-1 Nef contains a leucine-based motif located in a C-terminal unstructured loop that is required for both the interaction with clathrin-associated AP complexes and the Nef-mediated alterations of trafficking of most receptors, including CD4 (14,15,25). We therefore investigated the contribution of the leucine-based motif of Nef for its targeting into CCPs. Indeed, leucine-based motifs have been shown to drive clathrin-dependent internalization of several membrane proteins (20).

The role of this motif was first analyzed using the well-characterized Nef-LL/AA mutant, in which the two leucine residues were replaced by alanine. This mutant is impaired in several Nef functions including the downregulation of CD4, the upregulation of DC-SIGN and the perturbation of the recycling pathway. However, Nef-LL/AA efficiently mediates downregulation of MHC-I from the cell surface (10,13–15,21). The integrity of the di-leucine motif is also required for the Nef-mediated enhancement of viral infectivity (13,26). The distribution of the Nef-LL/AA mutant was therefore analyzed by TIR-FM imaging of living cells coexpressing the Nef-LL/AA–GFP fusion and DsRed-clathrin. The Nef-LL/AA mutant showed a diffuse staining at the plasma membrane with no evidence of concentration in CS (Figure 4A,B) compared with wild-type Nef (Figure 2). The impact of the LL/AA mutation was directly assessed by comparing the mean normalized fluorescence intensities inside CS of both wild-type Nef and Nef-LL/AA mutant. The mean fluorescence intensity of wild-type Nef inside CS was 1.27 (Figure 4G). In contrast, the mean fluorescence intensity of the LL/AA mutant dropped to 1.017 (Figure 4G), a value similar to background fluorescence. These results show that the Nef-LL/AA mutant is not concentrated in CS, indicating that the targeting of Nef into CCPs is dependent on the di-leucine AP-binding motif of Nef.

To further characterize the role of the native di-leucine ENTSLL sequence on Nef targeting to CCPs, we analyzed the effect of replacing this sequence of the Nef NL4-3 protein with leucine- or tyrosine-based endocytic motifs from cellular proteins. Previous analyses have shown that Nef variants containing di-leucine motifs, for example from the melanosomal tyrosinase (ERQPLL) or the from the γ chain of the T-cell receptor (DKQTLL), were almost fully active for CD4 downregulation and enhancement of viral infectivity (26). In contrast, those containing tyrosine-based motifs, for example from the TGN38 protein (SDYQRL), were as inactive as the Nef-LL/AA mutant. When imaged by TIR-FM, the Nef-ERQPLL and Nef-DKQTLL–GFP fusions were concentrated in spots and colocalized with DsRed-clathrin at the plasma membrane (Figure 4C,D and Figure S1, respectively), whereas the Nef-SDYQRL mutant exhibited a diffuse distribution similar to that of the Nef-LL/AA mutant (Figure 4B,F). Quantitative analysis of the images confirmed that the mean normalized fluorescence intensity of Nef-ERQPLL inside CS is equivalent to that measured for wild-type Nef (1.26 versus 1.27, respectively), while the mean intensity for Nef-SDYQRL was close to local background (1.015; Figure 4G). These results indicated that the di-leucine motif of Nef, required for the association to AP complexes, is also required for targeting of the protein into plasma membrane CCPs. Furthermore, this targeting can be mediated by a variety of leucine-based sequences but not by tyrosine-based AP-binding motifs.

CCP targeting of Nef di-leucine variants correlates with increased internalization of CD4

Our results indicate that Nef is constitutively enriched in CCPs and can be incorporated in forming CCVs. We next

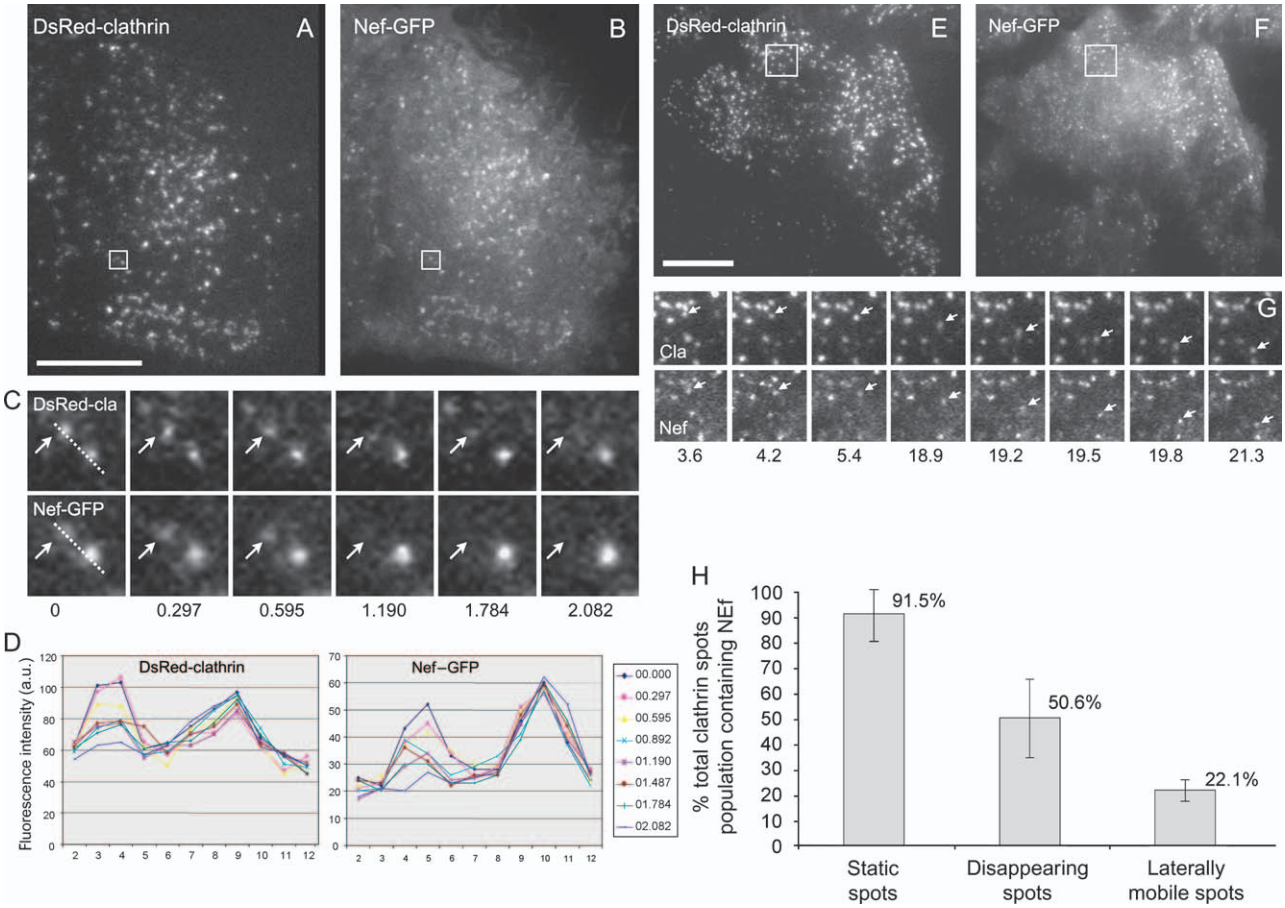

Figure 3: Distribution of Nef in dynamic CS populations. Live HeLa cells expressing DsRed-clathrin (A and E) and Nef–GFP (B and F) were imaged by TIR-FM acquired at ~300 mseconds/frame for 30 seconds. A–D) Distribution of Nef in disappearing CS. A disappearing spot was identified on the clathrin frame, then green and red images were separated, and the corresponding regions was magnified (×5, C). The fluorescence intensity of each marker was analyzed over time along a line drawn between two spots, a disappearing spot (arrow in C) and a static spot (D). The Nef- and clathrin-associated fluorescences decrease with the same kinetics in the disappearing spot while remaining stable in the neighboring static spot. E–G) Distribution of Nef in laterally mobile CS. A laterally mobile spot was identified on the clathrin frame, then green (F) and red images (E) were separated, and the corresponding region was magnified (×5, G). The upper panel corresponds to the clathrin images where a laterally mobile CS containing Nef–GFP (lower panel) was identified (arrows). Scale bars, 10 μm. H) Quantification. The presence of Nef–GFP inside 40 CS (from more than five cells) from each CS population (static, disappearing and laterally mobile) was determined using MetaMorph. Results are expressed as the percentage of CS of each population that contain Nef–GFP (normalized fluorescence >1.1).

asked whether the ability of Nef variants to be targeted to CCPs (Figure 4) correlated with their ability to affect steady-state distribution and/or internalization of CD4 from the cell surface in T cells. Therefore, HPB-ALL cells, a human T lymphoid cell line that endogenously expresses high level of CD4, were transiently transfected to express wild-type or mutated Nef–GFP fusions, and the effects on the levels of CD4 at the cell surface and CD4 internalization were quantified by flow cytometry (Figure 5). Expression of wild-type Nef decreased the levels of CD4 at the cell surface to 30% of control levels (Figure 5A) and highly stimulated internalization of CD4 from the plasma membrane (Figure 5B), leading to a sevenfold increase at 5 min compared with control nontransfected cells (Figure 5C). Cells expressing either Nef-LL/AA or Nef-SDYQRL, which failed to localize in CCPs, had steady-state CD4 surface levels and rates of CD4 internalization that were indistinguishable from control cells (Figure 5 and data not shown). The Nef-ERQPLL substitution mutant behaved similarly to wild-type Nef, with effective downmodulation and increased internalization of CD4 compared with LL/AA or SDYQRL mutants (Figure 5). However, the Nef-ERQPLL mutant was not as efficient as wild-type Nef. Indeed, Nef-ERQPLL-induced internalization of CD4 was lower than that by wild-type Nef at 5 min. Similarly, the Nef-ERQPLL-induced CD4 downregulation activity was slightly lower but significantly different ($p<0.05$) from that observed for wild-type Nef (Figure 5A).

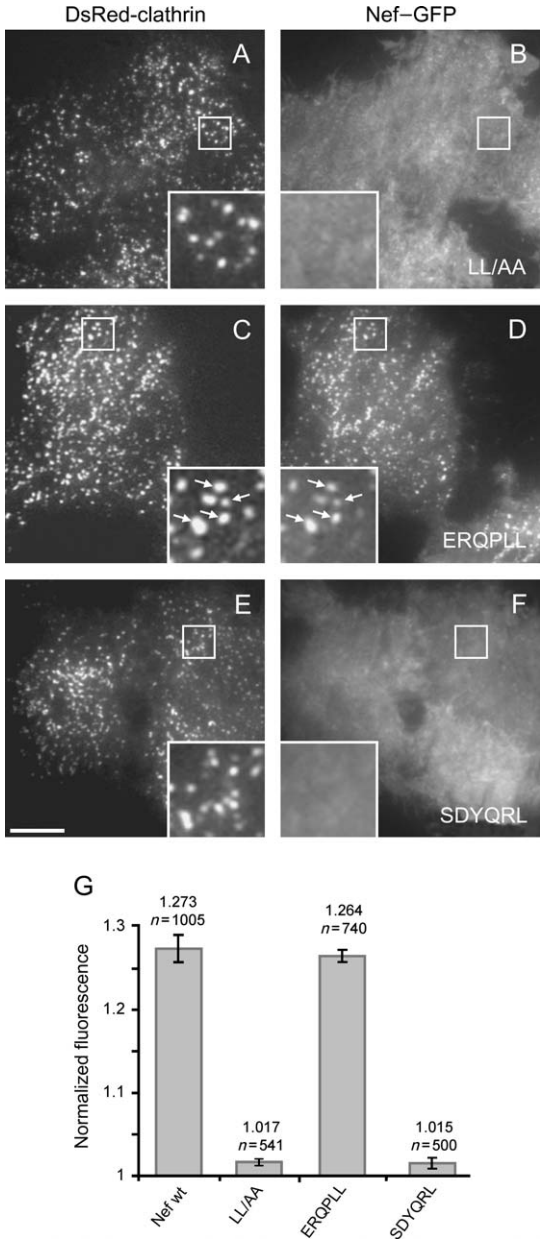

Figure 4: The di-leucine motif of Nef is required for colocalization with clathrin at the plasma membrane. Live HeLa cells expressing the LL/AA (A and B), ERQPLL (C and D) or SDYQRL (E and F) GFP-tagged Nef mutants in combination with DsRed-clathrin were imaged by TIR-FM as described in Figure 2. Insets show higher magnification (×3) of representative area and arrows indicate CS containing Nef. Scale bar, 10 μm. G) The mean normalized fluorescence intensity of each Nef variant within CS was quantified and compared with results obtained for wild-type (wt) Nef. The mean normalized fluorescence intensity was calculated for the number of spots indicated selected from four cells.

Altogether, the results reported in Figures 4 and 5 indicate that the leucine-based signal within the C-terminal loop of Nef is critical for both the targeting of the protein into CCP/CCVs and the stimulation of CD4 internalization.

Targeting to CCPs correlates with the Nef-induced internalization of CD4

The functions of Nef are not restricted to the stimulation of the endocytosis of CD4. Nef also disturbs the endosomal trafficking of multiple membrane-associated proteins and interferes with signal transduction in T cells through a Src homology 3 (SH3)-binding motif found in the N-terminal region of the protein. Although the Nef-mediated modulation of receptors such as CD4, CD28 and DC-SIGN requires the C-terminal AP-binding leucine-based motif (9,10,14,15), the downmodulation of MHC-I is determined by distinct motifs located in the N-terminal part of Nef: an acidic cluster (62EEEE65) and the SH3-binding motif (P72*XX*P75), involved in association with PACS-1 and Src-related tyrosine kinases, respectively (38–40). To analyze the contribution of these MHC-I-related motifs to the CCP targeting of Nef by TIR-FM, alanine substitutions were introduced in Nef–GFP. The substitution of the PXXP motif did not significantly affect the distribution of Nef at the plasma membrane, as evidenced by the concentration of the Nef-A72XXA75–GFP fusion in spots colocalizing with DsRed-clathrin (Figure 6A,B, arrows). The effective concentration of this mutant within CS was confirmed by a mean normalized fluorescence intensity higher than the local background (1.17; see Figure 6G). Despite its clear localization in CS, the A72XXA75 Nef mutant appeared less concentrated in CS than wild-type protein (1.17 versus 1.27; Figure 4G), but this slight difference did not affect the ability of the mutant protein to act on CD4. Indeed, the expression of the Nef-A72XXA75–GFP fusion downregulated the steady-state level and stimulated the internalization of CD4 from the cell surface as efficiently as the wild-type Nef–GFP fusion (Figure 7). Because we obtained similar results with a Nef-62EEEE65/4A–GFP fusion (data not shown), these results indicate that the motifs required for MHC-I downregulation are dispensable for targeting of Nef to CCP/CCV at the plasma membrane.

Finally, the model currently proposed for the Nef-induced endocytosis of CD4 postulates that Nef acts as a connector between AP complexes and CD4 [reviewed by Piguet and Trono (41)]. Whereas the recruitment of AP complexes is mediated by the di-leucine motif, the putative CD4-binding site was mapped by nuclear magnetic resonance (NMR) spectroscopy to residues found in the N-terminal part of Nef, including the tryptophan residue at position 57 (W57) (42). It was proposed that the substitution of W57 disrupts the binding of Nef to CD4 and therefore the Nef-mediated downregulation of CD4, without affecting the di-leucine motif-dependent recruitment of AP complexes (21). Indeed, a Nef-W57R–GFP fusion failed to downregulate CD4 or to stimulate its internalization from the cell surface of T cells (Figure 7). We tested the hypothesis that this region of Nef serves only as a CD4-binding site by analyzing the distribution of the mutated Nef-W57R–GFP fusion by TIR-FM. The distribution of the W57 mutant was compared with that of wild-type Nef and with that of a D123G mutant, which fails to form oligomers and is

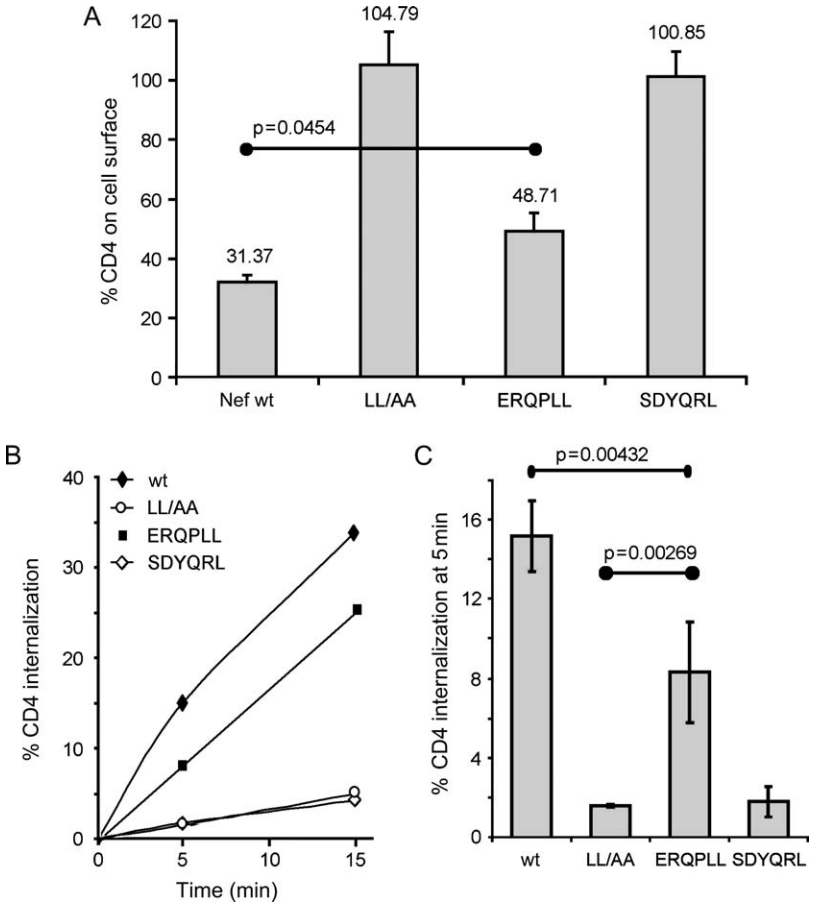

Figure 5: Downregulation and internalization of CD4 in T cells expressing Nef dileucine variants. HPB-ALL cells expressing wild-type (wt), LL/AA, ERQPLL or SDYQRL GFP-tagged Nef were assessed for CD4 cell surface expression at steady state (A) and internalization of CD4 (B and C) by flow cytometry. A) Cells were stained at 4°C with phycoerythrin (PE)-conjugated anti-CD4, and CD4-associated fluorescence was analyzed by flow cytometry on both GFP-positive and GFP-negative cells. Results are expressed as the percentage of the mean fluorescence intensity determined in GFP-positive cells relative to that determined in GFP-negative cells. B) After staining with PE-conjugated anti-CD4 antibody as indicated above, cells were incubated at 37°C for 0, 5 and 15 min to allow internalization. The percentage of internalization at each time-point was calculated as indicated in *Materials and Methods*. C) Percentages of internalization of CD4 at 5 min. Values are the means of three independent experiments. Error bars represent 1 standard deviation from the mean.

impaired for both downregulation of CD4 and MHC-I [(43); Figure 7 and data not shown]. Unexpectedly, the Nef-W57R–GFP fusion mutant showed a diffuse staining at the plasma membrane similar to that observed for the Nef-LL/AA–GFP and Nef-D123G–GFP fusions, with little if any concentration in CS (Figure 6D,F, arrowheads). The lack of concentration of the W57R and D123G mutants in CS was confirmed by quantitative analysis (Figure 6G); both mutants showed mean normalized fluorescence intensities close to the 1.1 limit value for clear observation of Nef-positive spots (1.10 and 1.08, respectively). These data indicated that the W57R mutant of Nef, predicted to be defective only in the ability to bind CD4, was defective in its targeting to CCP. These data also suggested that the oligomerization status of Nef is important for CCP targeting.

Altogether, the results reported in Figures 6 and 7 show a close correlation between localization of Nef to CCP and its ability to stimulate CD4 internalization from the plasma membrane.

CCP targeting of Nef is not affected by CD4 expression

In all the experiments described above, the distribution of Nef relative to that of clathrin was analyzed in HeLa cells and clearly showed that targeting of Nef into CS does not require CD4 expression but relies on its ability to interact with AP complexes (Figures 2, 4 and 6). However, in the connector model [see introductory paragraphs, and reviewed by Piguet and Trono (41)], Nef is believed to directly interact with the cytoplasmic tail of CD4 to mediate its internalization through the CCP/CCV pathway. In this model, expression of CD4 could be expected to influence the steady-state distribution of Nef at the plasma membrane. To test this hypothesis, we used HeLa cell lines stably expressing either wild-type CD4 or a mutant form of CD4 lacking its cytoplasmic region [CD4-wt and CD4-Δcyt, respectively, (44)]. Flow cytometry experiments confirmed that these two cell lines express similar high levels of CD4 at the cell surface (Figure 8A). Interestingly, it appeared from this analysis that all the cells from each cell line were found in an homogenous population in which every single cell did express CD4 as shown on the graph by the distribution of the cells within a single fluorescence pick (Figure 8 A). This was directly confirmed by immunofluorescence, showing cell surface CD4 staining for every cell (Figure 8B and data not shown). This observation was important for the single cell analysis of Nef distribution by TIR-FM (see below).

Before testing the distribution of Nef, we first checked the Nef effect on CD4 cell surface expression in both

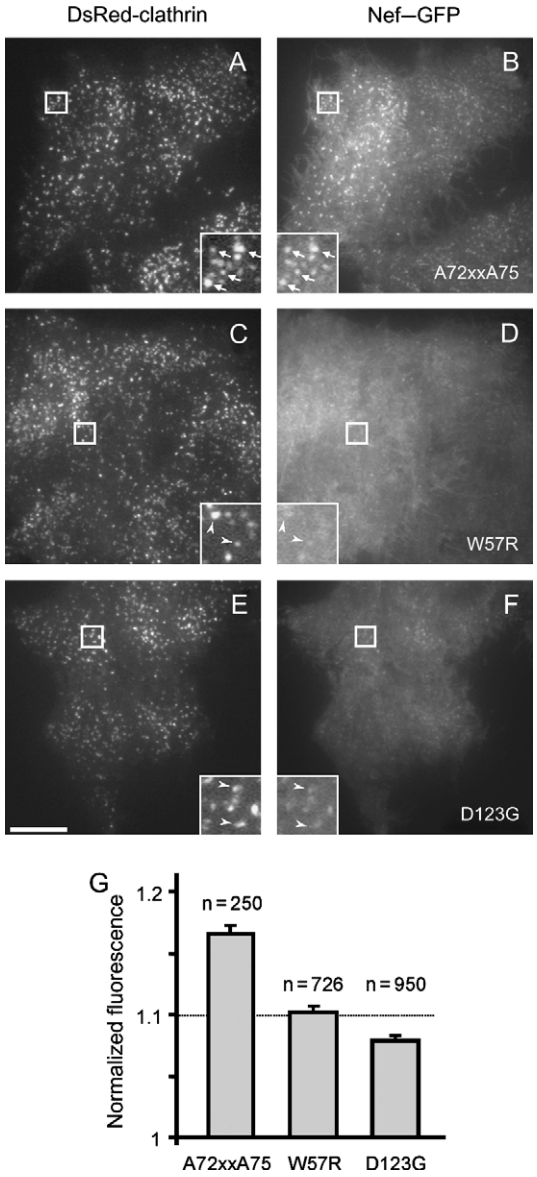

Figure 6: Distribution of Nef mutants at the plasma membrane. Live HeLa cells expressing A72XXA75 (A and B), W57R (C and D) or D123G (E and F) GFP-tagged Nef mutants in combination with DsRed-clathrin were imaged by TIR-FM as in Figures 2 and 4. Insets show higher magnification (×3) of representative area and arrows indicate CS containing Nef and arrowheads correspond to CS with low amounts of W57R and D123G Nef mutants. Scale bar, 10 μm. (G) The mean normalized fluorescence of each Nef variant within CS was quantified. The mean normalized fluorescence intensity was calculated for the number of spots indicated, which were selected from four cells.

HeLa-CD4-wt and HeLa-CD4-ΔCyt cell lines. As expected, Nef–GFP but not the LL/AA Nef mutant did reduce the steady-state CD4 cell surface staining in CD4-wt cells, whereas expression of wild-type or mutated Nef did not affect CD4 staining on the surface of CD4-Δcyt cells (Figure 8C). Finally, these two CD4-positive cell lines were cotransfected with Nef–GFP and DsRed-clathrin and analyzed by TIR-FM imaging. As illustrated in Figure 8D, the distribution of Nef at the plasma membrane was similar in the two cell lines and showed accumulation of Nef in spots colocalizing with clathrin. Quantification of the colocalization between the two markers showed that Nef was present in the large majority of CS present at the cell surface of CD4-wt or CD4-Δcyt cells (87 and 84.5%, respectively, see Figure 8E). The proportion of CS containing Nef was not significantly different between the two cell lines ($p = 0.24$), showing that the presence of Nef within clathrin-coated structures at the plasma membrane is not affected by CD4.

Discussion

The use of TIR-FM enables the first detailed dynamic analysis of the HIV-1 Nef protein at the plasma membrane of living cells. TIR-FM imaging shows that Nef is concentrated at the plasma membrane in spots that colocalize with clathrin-positive structures, and this distribution is independent of CD4 expression. Nef is distributed in both static and disappearing CS, which correspond to CCPs and forming vesicles (CCVs), respectively (33,34). In addition, the distribution of Nef in CCP/CCV correlates with its ability to stimulate CD4 internalization in T cells and is dependent on the presence of a functional leucine-based motif involved in Nef binding to AP complexes. Because this motif is also required for the maximal infectivity of HIV-1 virions (13,25,26), these results imply that the targeting of Nef to CCPs and CCVs participates in the Nef-mediated enhancement of viral infectivity.

Our results show that the HIV-1 Nef–GFP fusion is specifically enriched within clathrin-coated structures at the plasma membrane because the great majority if not all Nef-positive spots (>90%) detected by TIR-FM contain clathrin. While the majority (60%) of the clathrin structures were also positive for Nef, it is not clear whether the lack of a Nef–GFP signal in the remaining 40% results from insufficient sensitivity of detection or is related to a heterogeneous population of CS. Although previous studies have suggested that Nef may be partially associated with detergent-resistant membranes or 'rafts' at the plasma membrane, we failed to observe any overlap between Nef and caveolin-1 (data not shown), a marker of a raft-dependent non-clathrin pathway. This result is in agreement with a recent study, showing that functions of Nef at the plasma membrane do not depend on raft structures (45).

Our analysis of video streams showed that Nef is found in the three different populations of CS observable in live cells by TIR-FM. It is present in most (91.5%) of static CS that were previously characterized as CCPs that contain both clathrin and AP-2 complex (33,34). Nef is also found in 50.6% of the disappearing CS that correspond to forming CCVs. Although this value is likely underestimated by the observation that the intensity of clathrin is dimmer in the disappearing spots than in the static spots (37), this

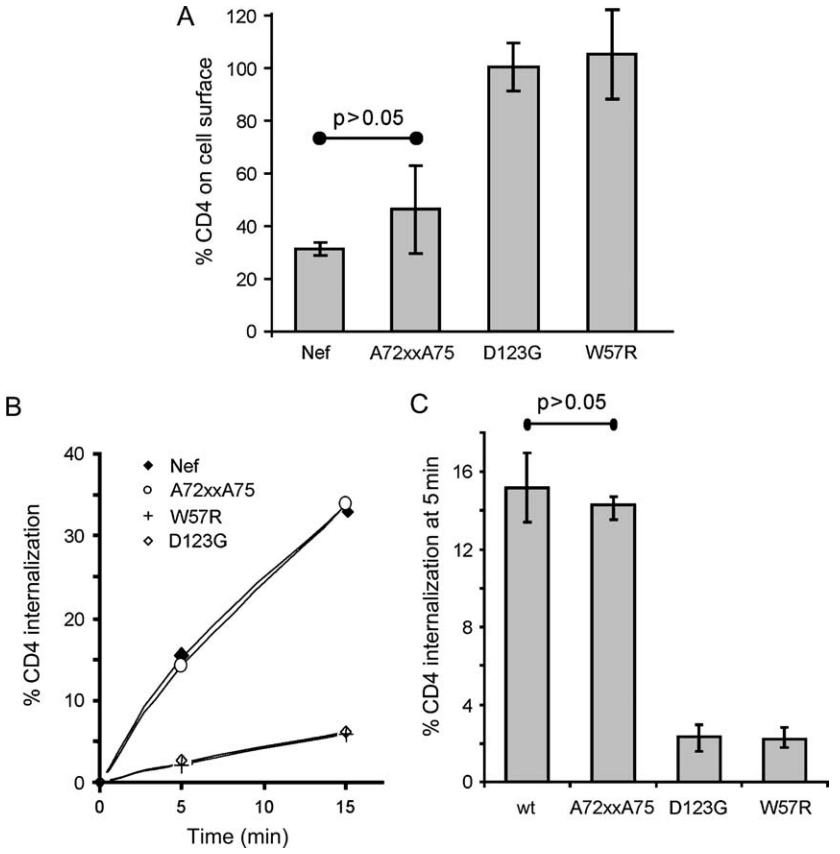

Figure 7: Downregulation and internalization of CD4 in cells expressing Nef mutants. HPB-ALL cells transiently expressing wild-type (wt), A72XXA75, W57R or D123G GFP-tagged Nef fusions were assessed for CD4 cell surface expression at steady state (A) and internalization of CD4 (B and C) as indicated in Figure 5. Values are the means of three independent experiments. Error bars represent 1 standard deviation from the mean.

indicates that Nef is also incorporated into forming vesicles. The presence of Nef in only half of the disappearing CS is not dissimilar to what we have recently found for epsin (unpublished observation), an adaptor for clathrin involved in CCV formation at the plasma membrane (46). Finally, Nef is present in laterally mobile CS; the function of such structures is not clear, but they may correspond to endosomal-associated clathrin coats [(33) and unpublished results]. Therefore, the detection of Nef–GFP within these laterally mobile structures may correspond to Nef on endosomes, where it is associated with AP-1 and AP-3 clathrin–adaptor complexes (27).

The observation that Nef was efficiently targeted to both CCPs and CCVs in HeLa cells suggested that CD4 was not directly involved in this process. Indeed, the hypothesis that CD4 would play an active role came from the model in which Nef functions as a specific 'connector' or 'adaptor' for CD4 driving its clathrin-dependent internalization through direct interaction with the CD4 cytoplasmic domain and the endocytic machinery [reviewed by Piguet and Trono (41)]. The results we obtained in this study clearly show that Nef was targeted to CCPs in the absence of CD4 (HeLa cells, Figure 2) and that Nef was similarly distributed in CCPs in cells stably expressing wild-type CD4 or a mutant form of CD4 lacking its cytoplasmic domain (Figure 8). These results paralleled those found for the Nef-induced perturbations of the early/sorting endosomal compartments that are also independent of CD4 expression and can be fully reproduced in cells that do not express CD4 (see below). Altogether, these results stress for a clear independence of Nef functions on the endocytic pathway relative to CD4 expression, in agreement with the increasing number of studies showing that Nef is able to perturb the trafficking of many different plasma membrane-associated proteins (8–13).

The accumulation of Nef in CS required the di-leucine motif found in the C-terminal solvent-exposed loop, which is also required for efficient binding to AP complexes. This latter result is in agreement with previous studies, which identified the di-leucine motif of Nef as the determinant required for efficient binding to AP complexes and colocalization with AP-2 in fixed cells (14,15). Our results show that this motif can be functionally replaced by leucine-based AP-binding motifs from heterologous cellular proteins but not by tyrosine-based motifs, even if the latter are also able to interact with AP complexes (26). This functional difference among endocytic motifs may be related to their different target subunits within AP complexes. Tyrosine-based motifs bind to the medium μ subunits (20), whereas leucine-based motifs were reported to bind to the $\gamma/\sigma1$ or $\delta/\sigma3$ hemicomplexes of AP-1 and AP-3 complexes (24,26) and/or to the β-adaptins (15,47). The finding that only leucine motifs are able to target Nef into CCPs suggests that binding to $\beta2$-adaptin or to the $\alpha/\sigma2$

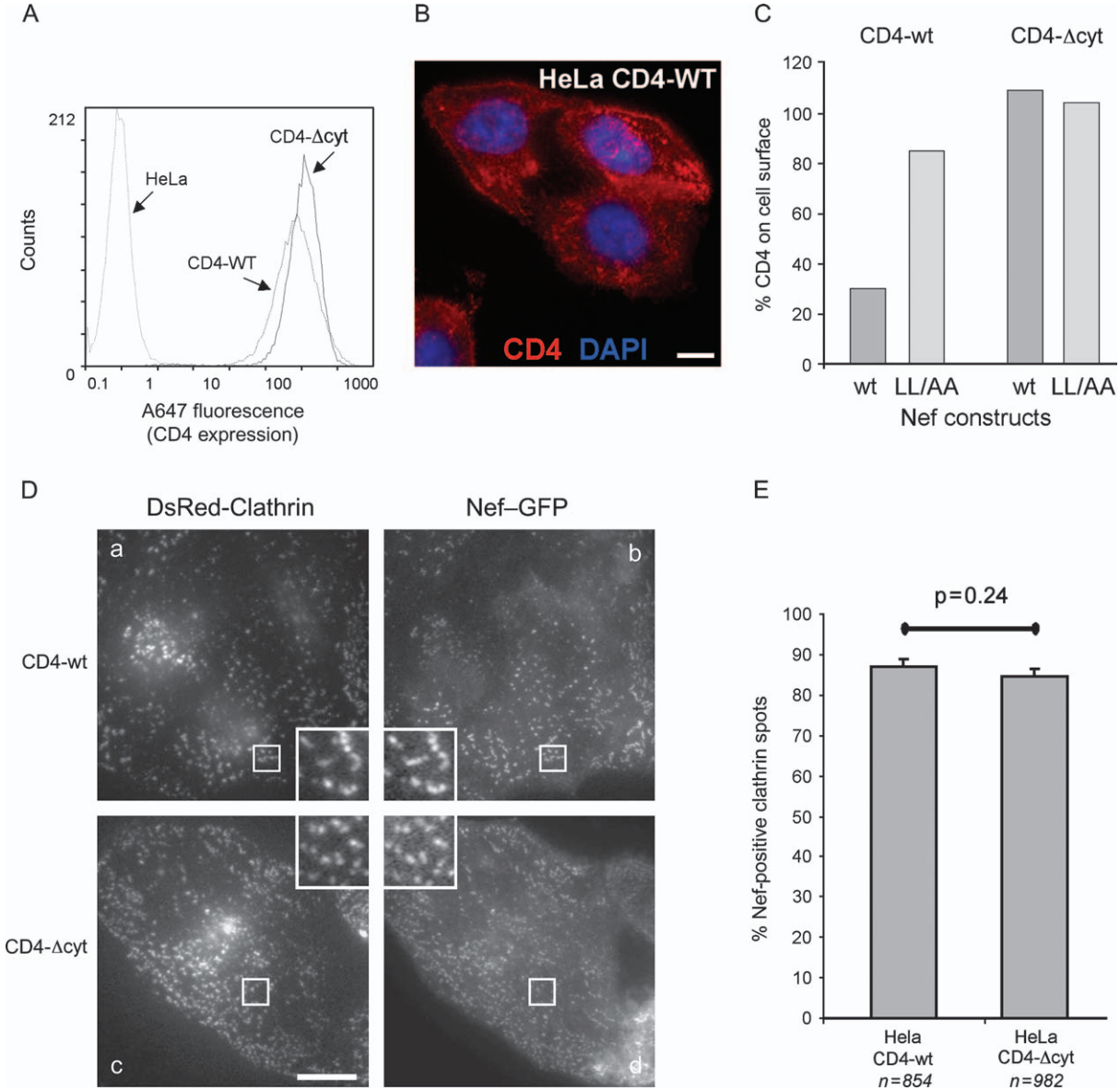

Figure 8: Colocalization of Nef with clathrin in HeLa cells stably expressing CD4. A and B) Cell surface expression of CD4. HeLa cells or HeLa cell lines stably expressing wild-type human CD4 (WT) or a mutant of CD4 with deletion of its cytoplasmic domain (Δcyt) were analyzed for CD4 cell surface expression by flow cytometry (A) or immunofluorescence (B) using anti-CD4 antibodies. C) Nef-induced CD4 downregulation. The effect of wild-type Nef and Nef-LL/AA mutant on cell surface CD4 expression was tested on HeLa-CD4-wt and HeLa-CD4-Δcyt cells, as described in Figures 5 and 7. D and E) Distribution of Nef in CD4-expressing cells. HeLa CD4-wt (D/a and b) or HeLa-CD4-Δcyt (D/c and d) cell lines transiently expressing DsRed-clathrin (D/a and c) and Nef–GFP (D/b and d) were analyzed by TIR-FM as shown in Figures 2, 4 and 6. Colocalization of Nef–GFP within CS (E) was quantified as described in Figure 2. Scale bars, 10 μm.

hemicomplex of AP-2 is necessary for localization in CCPs. Interestingly, both ARH (autosomal recessive hypercholesterolemia protein) and β-arrestins, APs specific for low-density lipoprotein (LDL) receptor family members and G protein-coupled receptors, respectively, are also targeted to CCPs through binding to β2-adaptin (48,49). However, Nef is also able to interact directly with the μ chains of AP complexes in a di-leucine independent manner. Thus, Nef is unusual in that it possesses distinct interfaces to mediate interactions with different subunits of the hetero-tetrameric AP complexes. Additional investigations are needed to understand the specific contributions and dynamics of these interactions.

Of note, Nef variants with heterologous leucine-based motifs are efficiently targeted to CCPs, but they are not fully functional (Figures 6 and 7). These results suggest that the endogenous ENTSLL signal of HIV-1 Nef may have attributes in addition to CCP targeting that confer maximal effects on CD4. Interestingly, the Nef variant containing

the ERQPLL motif from tyrosinase is less prevalent than wild-type Nef in disappearing CS but is more prevalent in laterally mobile CS (Figure S2). Because disappearing CS have been characterized as forming CCVs, this observation may explain why this Nef variant was slightly less efficient than the wild-type for CD4 internalization.

Nef profoundly disturbs the morphology and function of the early endosomal/recycling compartment (28–30). These effects may relate to its ability to recruit and stabilize the association of the clathrin-associated AP-1 and AP-3 complexes on endosomal membranes (27). Similarly, Nef could stabilize clathrin-coated structures containing AP-2 complexes at the plasma membrane, leading to an increase in the total number of CCPs. However, we found that the number of CS observable by TIR-FM at the cell surface was not significantly increased by the expression of Nef in HeLa cells that express or do not express CD4 (Figure S3). These results are partially in contrast to those of a previous study, which showed that the expression of Nef together with CD4, but not that of Nef alone, leads to an increase in the number of CCPs in B lymphocytes, which normally do not express CD4 (50). The difference in the effects of CD4 expression on Nef-induced formation of CCPs may be due to the different cell types used in the two studies (HeLa versus B lymphocytes). However, the results show that Nef is not able *per se* to drive CCP assembly at the plasma membrane.

The results also highlight an important difference between the effect of Nef at the plasma membrane and on endosomes because Nef markedly recruits both AP-1 and AP-3 adaptors (27) and clathrin (Figure 1) on endosomal membranes in a CD4-independent manner. Together with the observation that Nef expression does not affect the clathrin-dependent internalization of TfR even in CD4-positive T cells (13), these results suggest that Nef does not perturb the dynamics of the clathrin-mediated pathway at the plasma membrane but rather uses this pathway to trigger internalization of specific surface receptors. In contrast, the Nef-induced membrane stabilization of AP-1 and AP-3 on early/sorting endosomes severely perturbs the function of the recycling compartment and leads to an inhibition of the recycling of CD4 and TfR to the cell surface (6,13). Interestingly, HIV-1 Nef binds very weakly to intact AP-2, whereas a relatively robust binding to intact AP-1 and AP-3 has been detected (5,14,15,24,51). These features may explain the differential impact of Nef on the AP-2 and AP-1/AP-3 pathways and suggest that Nef associates with these complexes through distinct molecular mechanisms.

The role of CCP localization on the function of Nef was investigated by testing the impact of Nef variants on CD4 endocytosis. In T lymphocytes, CD4 is primarily present at the cell surface and is only slowly internalized, but the expression of Nef strongly stimulates the endocytosis of CD4. As expected, the ability of Nef variants to reduce CD4 expression at the cell surface and to stimulate the internalization of CD4 correlated closely with their ability to accumulate in CCPs, suggesting that localization of Nef in CCPs and forming CCVs is required to induce the internalization of CD4. These results are in agreement with a recent study showing that Nef-induced downmodulation of CD4 in T lymphoid cells can be related to the clathrin-mediated endocytic pathway and is directly dependant on AP-2 expression (32).

The current molecular model for the action of Nef on CD4 suggests that Nef acts as a connector between the CD4 and the clathrin-associated AP-2 complex at the plasma membrane [reviewed by Piguet et al. (7)]. This connection would result in the targeting of CD4 to CCPs for rapid internalization via CCVs. Thus, Nef is expected to play a role similar to that of cargo-specific adaptors such as β-arrestin and ARH, which connect G protein-coupled receptors or LDL receptors to AP-2 (48,49). In this connector model, two distinct regions of Nef are involved in the recruitment of CD4 and in the binding to AP complexes. Whereas the recruitment of AP complexes is mediated by the C-terminal di-leucine motif of Nef (see above), the putative CD4-binding site is found in the N-terminal part of the protein and includes residue W57 (42). The fact that W57 mutants of Nef were affected in their ability to downregulate CD4 was then interpreted as an argument in favor of the connector model (7). However, our present observations show that the W57R mutant is not concentrated in clathrin-coated structures at the plasma membrane (Figure 6), in agreement with a previous study showing that mutation of W57 impaired colocalization of Nef with AP-2 complexes in fixed cells (35). Together, these results indicate that mutation of the W57 affects the interaction of Nef with both CD4 and the clathrin-dependent machinery. It remains to be determined if the W57 residue is directly involved in the interaction with AP complexes or if it is important for the general folding of the molecule as it was suggested by structural studies (52). The observation that the W57 mutants of Nef failed to localize in CCPs stresses that the results obtained with these mutants could not be simply interpreted as a consequence of a specific loss of interaction with CD4. However, the finding that the W57 residue of Nef is also important for efficient targeting in CCPs does not definitively argue against the Nef connector model but indicates that more specific Nef mutants are needed to properly evaluate this model.

The connector model has recently been challenged by the observations that the leucine motif of CD4, although required for Nef-induced internalization (3), is not required for the binding to Nef (53,54). These observations suggest an alternative model in which the leucine motif of CD4 participates directly in the binding to AP complexes during Nef-mediated downregulation. Interestingly, a recent study showed that Nef induces the relocalization of the CD4-associated kinase Lck from the plasma membrane toward intracellular compartments (55). One intriguing possibility is then that Nef may induce dissociation of CD4

from Lck, therefore allowing its internalization. However, the fact that the mislocalization of Lck was also observed with the LL/AA mutant of Nef (55) suggests that mislocalization of Lck and CD4 downregulation activities of Nef are not related events. Finally, in an alternative model, Nef functions as a general 'troublemaker' of the endocytic pathway affecting the intracellular trafficking of not only membrane proteins including of course CD4 but also many other plasma membrane-associated proteins (see introductory paragraphs). The latter model being not exclusive of the connector one, the way Nef is exactly acting on CD4 appears then far from being clarified.

Another possibility that is not mutually exclusive with the 'connector' function is that Nef may use the classical clathrin-dependent internalization pathway to reach the early/sorting endosomes. Once within the endosomal system, Nef induces morphological and functional disturbances that affect not only early/recycling endosomes but also late endosomes and multivesicular bodies (28–30). How Nef trafficks within the endosomal system to reach the perinuclear endosomal region where it is concentrated at steady state is not understood. In this regard, chimeras in which Nef is fused to the extracellular and transmembrane domains of an integral membrane protein, such as CD4 or CD8, are constitutively internalized, and the leucine motif of Nef is critical for this internalization (4,6,16,29). Furthermore, the ENTSLL sequence of HIV-1 Nef functions as an endocytic signal when appended to the cytoplasmic tail of a heterologous transmembrane protein (14,25). These findings provide definitive evidence that the leucine-based motif of Nef acts as an internalization signal *per se*. Here, the detection of Nef–GFP in at least 50% of forming CCVs likely *en route* to the early/sorting endosomes, confirms that Nef present at the plasma membrane uses the clathrin-mediated pathway to concentrate in the endosomal compartments, where it may promote the formation of a platform for assembly of HIV-1 virions by inducing an expansion of multivesicular endosomal structures.

In conclusion, our data show that Nef is present at the cell surface in both CCPs and forming vesicles. This distribution correlates with the Nef-induced stimulation of CD4 endocytosis and is strictly dependent on the di-leucine AP-binding motif of Nef. These findings confirm a model in which Nef initially uses the clathrin-mediated endocytic pathway to induce the rapid internalization of some transmembrane proteins, such as CD4, from the surface of HIV-1-infected cells.

Materials and Methods

Plasmids

Vectors for expression of Nef from HIV-1 NL4-3 fused to GFP (Nef–GFP) as well as the LL/AA Nef mutant were described previously (13). The previously described EERQPLL, DKQTLL and SDYQRL Nef variants were constructed as GFP fusions by exchanging the Nef-coding sequence in pCG-GFP (35) with that from pCINef-EERQPLL, -DKQTLL and -SDYQRL (26) using appropriate restriction sites within *nef*. The W57R and D123G GFP-tagged mutants were generated in this study by polymerase chain reaction-directed mutagenesis using appropriate primers as described (13). Clathrin light chain fused to DsRed was a gift of Dr Thomas Kirchhausen (Harvard Medical School, Boston, MA, USA). The caveolin-1 protein fused to mRFP (monomeric form of red fluorescent protein) (Cav1-mRFP) was a kind gift from Dr Richard Pagano [Mayo Clinic and Foundation, Rochester, MN, USA; (56)].

Cell culture and transfection

HeLa cells were maintained in DMEM (Mediatech Cellgro, Herndon, VA, USA or Invitrogen, Cergy Pontoise, France) with 10% fetal calf serum (FCS) in a 37°C incubator humidified with 5% CO_2. HeLa cell lines stably expressing wild-type CD4 or a mutant form of CD4 lacking the cytoplasmic domain [CD4-wt and CD4-Δcyt, respectively (44)] were maintained in DMEM containing 4% FCS supplemented with 1 mg/mL Geneticin sulfate (G418; Invitrogen). Cells were imaged approximately 40 h after transfection with Fugene6 (Roche Diagnostics, Indianapolis, IN, USA) or with Genejuice (Novagen, VWR, Fontenay sous bois, France). CD4-positive human peripheral blood–acute lymphocytic leukemia (HPB-ALL) cells were kindly provided by G. Bismuth (Institut Cochin, Paris, France) and were maintained in RPMI-1640 medium with Glutamax-1 supplemented with 10% FCS (Invitrogen). HPB-ALL cells were transfected by electroporation as previously described (57) and both the cell surface level at steady state and the rate of internalization of CD4 were assessed 24 h after transfection.

Fluorescence microscopy and image acquisition

Total internal reflection fluorescence microscopy was performed as previously described (37) using an Apo 60X NA 1.45 microscope objective with an inverted epifluorescence microscope (IX-70, Olympus; Olympus America Inc., Melville, NY, USA) placed within a home-built temperature-controlled enclosure set at 37°C for live cell imaging. To image simultaneously both DsRed-clathrin and HIV-1 Nef–GFP fusions, both fluorophores were excited with the 488 nm line of the same tunable Argon laser (Omnichrome, model 543-AP A01; Melles Griot, Carlsbad, CA, USA) reflected off the 498dclp dichroic mirror. Image acquisition was performed using an emission splitter (DualView; Optical Insights, Santa Fe, NM, USA) with the images focused simultaneously onto an ORCA ER cooled charge-coupled device (CCD) (Hamamatsu Photonics, Hamamatsu City, Japan). The GFP/DsRed emissions were collected simultaneously through an emission splitter equipped with dichroic mirrors to split the emission (550dc, long pass filter). The GFP emission was then collected through an emission band pass filter (HQ525/50 nm) and the DsRed emission through an emission long pass filter (580 nm). All mirrors and filters were obtained from Chroma Technologies Corp. (Brattleboro, VT, USA). Streams of 100–300 frames were acquired at ~300 mseconds per frame.

For epifluorescence, classical HeLa cells transiently transfected with both DsRed-clathrin and Nef–GFP were fixed in paraformaldehyde for 30 min at 4°C and mounted on microscope slides in PBS/glycerol (50/50). For cell surface CD4 staining, HeLa cell lines expressing CD4 were first incubated with purified anti-CD4 antibody (clone SK3; BD Biosciences, Le Pont de Claix, France) in PBS-BSA (PBS supplemented with BSA, 1 mg/mL) at 4°C for 1 h. Cells were then washed in cold PBS and then fixed and processed as described above. Fixed cells were finally examined under an epifluorescence microscope (Leica, Rueil-Malmaison, France) attached to a cooled CCD camera (Micromax; Roper Scientific, Evry, France).

The shutters, filters and camera as well as acquisition were controlled by MetaMorph (Molecular Dynamics, Downingtown, PA, USA). The final images were generated using National Institutes of Health (NIH) image (http://rsb.info.nih.gov/nih-image/) or scion image (http://www.scioncorp.com) and Photoshop (Adobe Systems Inc, San Jose, CA, USA).

Image analysis using MetaMorph

Following the subtraction of extracellular background, 12-bit dual-color TIR-FM image streams were aligned using a journal written for MetaMorph

(Universal Imaging, Downingtown, PA, USA). On the basis of controls using single fluorophores (37), green to red bleed through corrections of 10% for HIV-1 Nef–GFP and clathrin-DsRed were used. To calculate the mean normalized fluorescence of Nef–GFP inside DsRed-CS, individual CS was circled using MetaMorph. The resulting regions were transferred to the Nef images, and the fluorescence intensity corresponding to GFP inside these regions was measured; this represented the fluorescence intensity of Nef inside CS. To normalize these values to the local background, the regions were shifted on the clathrin images to select equivalent regions outside CS. Then, the resulting regions were transferred on the Nef images. The average of the value obtained for GFP fluorescence inside these shifted regions represents the background fluorescence of GFP outside CS. The fluorescence intensity of Nef–GFP inside CS was divided by the average of the fluorescence of GFP outside CS to obtain the mean normalized fluorescence intensity inside CS.

Flow cytometry analysis

Steady-state cell surface levels of CD4 and its rate of internalization were assessed in HPB-ALL cells transfected by electroporation with plasmids expressing the Nef–GFP fusions. Twenty hours after transfection, cells were washed with cold washing buffer (PBS supplemented with BSA, 5 mg/mL) and labeled for 1 h at 4°C with a phycoerythrin-conjugated or alexa-647 anti-CD4 antibody (SK3 clone, used at 1/10 dilution; BD Biosciences, Le Pont de Claix, France) in cold washing buffer. Cells were then washed in cold washing buffer and then incubated at 37°C for 0, 5, 15 or 45 min (internalization) in washing buffer or kept at 4°C in PBS (maximum cell surface staining). After internalization, cells were again washed in cold washing buffer and cell surface-bound anti-CD4 antibody was then stripped by a 75-second incubation at 4°C in an acidic buffer (50 mM glycine, 100 mM NaCl, pH 4). Cells were washed in cold PBS and then fixed in PBS, 2% formaldehyde and 0.1% azide. Cell-associated CD4 staining was measured by flow cytometry (Cytomics FC 500; Beckman Coulter, Villepinte, France; flow cytometry facility of the Cochin Institute) in either GFP-positive or GFP-negative cells. The percentage of CD4 that was downregulated was calculated by comparing the maximal cell surface CD4 staining (no internalization, no stripping) in Nef–GFP-expressing cells with the staining measured for the GFP-negative cells within the same tube. The percentage of internalized CD4 was calculated as follows: $[(m_X - m_0)/(m_T - m_0)] \times 100$, where m_X is the mean fluorescence obtained at each time-point, m_0 is the mean fluorescence obtained at time zero after acid wash and m_T is the total mean fluorescence obtained at time zero (without acid wash).

Acknowledgments

This work was supported by 'Agence Nationale de Recherche sur le SIDA' and SIDACTION (S. B.), NIH 1 F32 GM069200-02 (J. Z. R.), NSF BES-0110070, NIH AI38201 (J. C. G.) and BES-0119468 (S. M. S.). The authors thank Thomas Kirchhausen and Richard E. Pagano for providing the DsRed-tagged clathrin and mRFP1-tagged caveolin constructs, respectively, and Annegret Pelchen-Matthews and Mark Marsh for their generous gift of CD4-expressing HeLa cell lines and people from the Institut Cochin Facilities (Plateformes de séquençage et de cytométrie en flux).

Supplementary Material

Figure S1: Nef-DKQTLL mutant colocalizes with clathrin at the plasma membrane. HeLa cells transiently expressing the DKQTLL Nef substitution mutant (A) and DsRed-clathrin (B) were imaged by TIR-FM as in Figure 2. Insets show higher magnification of a representative area and arrows stress colocalizing spots. Scale bar, 10 μm.

Figure S2: Distribution of the Nef-ERQPLL mutant within dynamic CS populations. Live HeLa cells expressing either wild-type (black bars) or ERQPLL (gray bars) GFP-tagged Nef fusions in combination with DsRed-clathrin were imaged by TIR-FM. The presence of Nef–GFP inside 40 CS (from more than five cells) from each CS population was determined using MetaMorph. Results are expressed as the percentage of CS of each population that contain Nef (Figure 3).

Figure S3: Expression of Nef does not increase the number of CS at the plasma membrane. HeLa cells transiently expressing wild-type (blue) or LL/AA (white) Nef-GFP fusion together with DsRed-clathrin, or CD4-wt (red) or CD4-Δcyt (gray) HeLa cell lines expressing Nef–GFP fusions together with DsRed-clathrin were imaged by TIR-FM. For each cell ($n = 4$), the total number of CS present at the adherent membrane was quantified and then normalized to arbitrary surface unit.

Video S1: Time-lapse movie showing a disappearing spot imaged by TIR-FM, which contained both clathrin (top) and Nef (bottom). ~0.3 second/frame.

Video S2: Time-lapse movie showing a laterally mobile spot imaged by TIR-FM, which contained both clathrin (top) and Nef (bottom). ~0.3 second/frame.

Supplemental materials are available as part of the online article at http://www.blackwell-synergy.com

References

1. Fackler OT, Baur AS. Live and let die: Nef functions beyond HIV replication. Immunity 2002;16:493–497.
2. Wei BL, Arora VK, Foster JL, Sodora DL, Garcia JV. In vivo analysis of Nef function. Curr HIV Res 2003;1:41–50.
3. Aiken C, Konner J, Landau NR, Lenburg ME, Trono D. Nef induces CD4 endocytosis: requirement for a critical dileucine motif in the membrane-proximal CD4 cytoplasmic domain. Cell 1994;76:853–864.
4. Mangasarian A, Foti M, Aiken C, Chin D, Carpentier JL, Trono D. The HIV-1 Nef protein acts as a connector with sorting pathways in the Golgi and at the plasma membrane. Immunity 1997;6:67–77.
5. Le Gall S, Erdtmann L, Benichou S, Berlioz-Torrent C, Liu L, Benarous R, Heard JM, Schwartz O. Nef interacts with the mu subunit of clathrin adaptor complexes and reveals a cryptic sorting signal in MHC I molecules. Immunity 1998;8:483–495.
6. Piguet V, Gu F, Foti M, Demaurex N, Gruenberg J, Carpentier JL, Trono D. Nef-induced CD4 degradation: a diacidic-based motif in Nef functions as a lysosomal targeting signal through the binding of beta-COP in endosomes. Cell 1999;97:63–73.
7. Piguet V, Schwartz O, Le Gall S, Trono D. The downregulation of CD4 and MHC-I by primate lentiviruses: a paradigm for the modulation of cell surface receptors. Immunol Rev 1999;168:51–63.
8. Stumptner-Cuvelette P, Morchoisne S, Dugast M, Le Gall S, Raposo G, Schwartz O, Benaroch P. HIV-1 Nef impairs MHC class II antigen presentation and surface expression. Proc Natl Acad Sci U S A 2001;98:12144–12149.
9. Swigut T, Shohdy N, Skowronski J. Mechanism for down-regulation of CD28 by Nef. EMBO J 2001;20:1593–1604.
10. Sol-Foulon N, Moris A, Nobile C, Boccaccio C, Engering A, Abastado JP, Heard JM, van Kooyk Y, Schwartz O. HIV-1 Nef-induced upregulation of DC-SIGN in dendritic cells promotes lymphocyte clustering and viral spread. Immunity 2002;16:145–155.
11. Hrecka K, Swigut T, Schindler M, Kirchhoff F, Skowronski J. Nef proteins from diverse groups of primate lentiviruses downmodulate CXCR4 to inhibit migration to the chemokine stromal derived factor 1. J Virol 2005;79:10650–10659.

12. Michel N, Allespach I, Venzke S, Fackler OT, Keppler OT. The Nef protein of human immunodeficiency virus establishes superinfection immunity by a dual strategy to downregulate cell-surface CCR5 and CD4. Curr Biol 2005;15:714–723.
13. Madrid R, Janvier K, Hitchin D, Day J, Coleman S, Noviello C, Bouchet J, Benmerah A, Guatelli J, Benichou S. Nef-induced alteration of the early/recycling endosomal compartment correlates with enhancement of HIV-1 infectivity. J Biol Chem 2005;280:5032–5044.
14. Bresnahan PA, Yonemoto W, Ferrell S, Williams-Herman D, Geleziunas R, Greene WC. A dileucine motif in HIV-1 Nef acts as an internalization signal for CD4 downregulation and binds the AP-1 clathrin adaptor. Curr Biol 1998;8:1235–1238.
15. Greenberg M, DeTulleo L, Rapoport I, Skowronski J, Kirchhausen T. A dileucine motif in HIV-1 Nef is essential for sorting into clathrin--coated pits and for downregulation of CD4. Curr Biol 1998;8: 1239–1242.
16. Lu X, Yu H, Liu SH, Brodsky FM, Peterlin BM. Interactions between HIV1 Nef and vacuolar ATPase facilitate the internalization of CD4. Immunity 1998;8:647–656.
17. Piguet V, Wan L, Borel C, Mangasarian A, Demaurex N, Thomas G, Trono D. HIV-1 Nef protein binds to the cellular protein PACS-1 to downregulate class I major histocompatibility complexes. Nat Cell Biol 2000;2:163–167.
18. Blagoveshchenskaya AD, Thomas L, Feliciangeli SF, Hung CH, Thomas G. HIV-1 Nef downregulates MHC-I by a PACS-1- and PI3K-regulated ARF6 endocytic pathway. Cell 2002;111:853–866.
19. Robinson MS. Adaptable adaptors for coated vesicles. Trends Cell Biol 2004;14:167–174.
20. Bonifacino JS, Traub LM. Signals for sorting of transmembrane proteins to endosomes and lysosomes. Annu Rev Biochem 2003;72:395–447.
21. Mangasarian A, Piguet V, Wang JK, Chen YL, Trono D. Nef-induced CD4 and major histocompatibility complex class I (MHC-I) down-regulation are governed by distinct determinants: N-terminal alpha helix and proline repeat of Nef selectively regulate MHC-I trafficking. J Virol 1999;73:1964–1973.
22. Riggs NL, Craig HM, Pandori MW, Guatelli JC. The dileucine-based sorting motif in HIV-1 Nef is not required for down-regulation of class I MHC. Virology 1999;258:203–207.
23. Craig HM, Reddy TR, Riggs NL, Dao PP, Guatelli JC. Interactions of HIV-1 nef with the mu subunits of adaptor protein complexes 1, 2, and 3: role of the dileucine-based sorting motif. Virology 2000;271:9–17.
24. Janvier K, Kato Y, Boehm M, Rose JR, Martina JA, Kim BY, Venkatesan S, Bonifacino JS. Recognition of dileucine-based sorting signals from HIV-1 Nef and LIMP-II by the AP-1 gamma-sigma1 and AP-3 delta-sigma3 hemicomplexes. J Cell Biol 2003;163:1281–1290.
25. Craig HM, Pandori MW, Guatelli JC. Interaction of HIV-1 Nef with the cellular dileucine-based sorting pathway is required for CD4 down-regulation and optimal viral infectivity. Proc Natl Acad Sci U S A 1998;95:11229–11234.
26. Coleman SH, Van Damme N, Day JR, Noviello CM, Hitchin D, Madrid R, Benichou S, Guatelli JC. Leucine-specific, functional interactions between human immunodeficiency virus type 1 Nef and adaptor protein complexes. J Virol 2005;79:2066–2078.
27. Janvier K, Craig H, Hitchin D, Madrid R, Sol-Foulon N, Renault L, Cherfils J, Cassel D, Benichou S, Guatelli J. HIV-1 Nef stabilizes the association of adaptor protein complexes with membranes. J Biol Chem 2003;278:8725–8732.
28. Sanfridson A, Hester S, Doyle C. Nef proteins encoded by human and simian immunodeficiency viruses induce the accumulation of endosomes and lysosomes in human T cells. Proc Natl Acad Sci U S A 1997; 94:873–878.
29. Erdtmann L, Janvier K, Raposo G, Craig HM, Benaroch P, Berlioz-Torrent C, Guatelli JC, Benarous R, Benichou S. Two independent regions of HIV-1 Nef are required for connection with the endocytic pathway through binding to the mu 1 chain of AP1 complex. Traffic 2000; 1:871–883.
30. Stumptner-Cuvelette P, Jouve M, Helft J, Dugast M, Glouzman AS, Jooss K, Raposo G, Benaroch P. Human immunodeficiency virus-1 Nef expression induces intracellular accumulation of multivesicular bodies and major histocompatibility complex class II complexes: potential role of phosphatidylinositol 3-kinase. Mol Biol Cell 2003;14: 4857–4870.
31. Bresnahan PA, Yonemoto W, Greene WC. Cutting edge: SIV Nef protein utilizes both leucine- and tyrosine-based protein sorting pathways for down-regulation of CD4. J Immunol 1999;163:2977–2981.
32. Jin YJ, Cai CY, Zhang X, Zhang HT, Hirst JA, Burakoff SJ. HIV Nef-mediated CD4 down-regulation is adaptor protein complex 2 dependent. J Immunol 2005;175:3157–3164.
33. Rappoport J, Simon S, Benmerah A. Understanding living clathrin-coated pits. Traffic 2004;5:327–337.
34. Perrais D, Merrifield CJ. Dynamics of endocytic vesicle creation. Dev Cell 2005;9:581–592.
35. Greenberg ME, Bronson S, Lock M, Neumann M, Pavlakis GN, Skowronski J. Co-localization of HIV-1 Nef with the AP-2 adaptor protein complex correlates with Nef-induced CD4 down-regulation. EMBO J 1997;16:6964–6976.
36. Rappoport JZ, Taha BW, Lemeer S, Benmerah A, Simon SM. The AP-2 complex is excluded from the dynamic population of plasma membrane-associated clathrin. J Biol Chem 2003;278:47357–47360.
37. Rappoport JZ, Benmerah A, Simon SM. Analysis of the AP-2 adaptor complex and cargo during clathrin-mediated endocytosis. Traffic 2005;6:539–547.
38. Greenberg ME, Iafrate AJ, Skowronski J. The SH3 domain-binding surface and an acidic motif in HIV-1 Nef regulate trafficking of class I MHC complexes. EMBO J 1998;17:2777–2789.
39. Crump CM, Xiang Y, Thomas L, Gu F, Austin C, Tooze SA, Thomas G. PACS-1 binding to adaptors is required for acidic cluster motif-mediated protein traffic. EMBO J 2001;20:2191–2201.
40. Saksela K, Cheng G, Baltimore D. Proline-rich (PxxP) motifs in HIV-1 Nef bind to SH3 domains of a subset of Src kinases and are required for the enhanced growth of Nef+ viruses but not for down-regulation of CD4. EMBO J 1995;14:484–491.
41. Piguet V, Trono D. The Nef protein of primate lentiviruses. Rev Med Virol 1999;9:111–120.
42. Grzesiek S, Stahl SJ, Wingfield PT, Bax A. The CD4 determinant for downregulation by HIV-1 Nef directly binds to Nef. Mapping of the Nef binding surface by NMR. Biochemistry 1996;35:10256–10261.
43. Liu LX, Heveker N, Fackler OT, Arold S, Le Gall S, Janvier K, Peterlin BM, Dumas C, Schwartz O, Benichou S, Benarous R. Mutation of a conserved residue (D123) required for oligomerization of human immunodeficiency virus type 1 Nef protein abolishes interaction with human thioesterase and results in impairment of Nef biological functions. J Virol 2000;74:5310–5319.
44. Pitcher C, Honing S, Fingerhut A, Bowers K, Marsh M. Cluster of differentiation antigen 4 (CD4) endocytosis and adaptor complex binding require activation of the CD4 endocytosis signal by serine phosphorylation. Mol Biol Cell 1999;10:677–691.
45. Sol-Foulon N, Esnault C, Percherancier Y, Porrot F, Metais-Cunha P, Bachelerie F, Schwartz O. The effects of HIV-1 Nef on CD4 surface expression and viral infectivity in lymphoid cells are independent of rafts. J Biol Chem 2004;279:31398–31408.
46. Chen H, Fre S, Slepnev VI, Capua MR, Takei K, Butler MH, Di Fiore PP, De Camilli P. Epsin is an EH-domain-binding protein implicated in clathrin-mediated endocytosis. Nature 1998;394:793–797.
47. Rapoport I, Chen YC, Cupers P, Shoelson SE, Kirchhausen T. Dileucine-based sorting signals bind to the beta chain of AP-1 at a site distinct and

regulated differently from the tyrosine-based motif-binding site. EMBO J 1998;17:2148–2155.
48. Mishra SK, Keyel PA, Edeling MA, Dupin AL, Owen DJ, Traub LM. Functional dissection of an AP-2 beta2 appendage-binding sequence within the autosomal recessive hypercholesterolemia protein. J Biol Chem 2005;280:19270–19280.
49. Laporte SA, Oakley RH, Holt JA, Barak LS, Caron MG. The interaction of beta-arrestin with the AP-2 adaptor is required for the clustering of beta 2-adrenergic receptor into clathrin-coated pits. J Biol Chem 2000;275:23120–23126.
50. Foti M, Mangasarian A, Piguet V, Lew DP, Krause KH, Trono D, Carpentier JL. Nef-mediated clathrin-coated pit formation. J Cell Biol 1997;139:37–47.
51. Piguet V, Chen YL, Mangasarian A, Foti M, Carpentier JL, Trono D. Mechanism of Nef-induced CD4 endocytosis: Nef connects CD4 with the mu chain of adaptor complexes. EMBO J 1998;17:2472–2481.
52. Grzesiek S, Bax A, Hu JS, Kaufman J, Palmer I, Stahl SJ, Tjandra N, Wingfield PT. Refined solution structure and backbone dynamics of HIV-1 Nef. Protein Sci 1997;6:1248–1263.
53. Bentham M, Mazaleyrat S, Harris M. The di-leucine motif in the cytoplasmic tail of CD4 is not required for binding to human immunodeficiency virus type 1 Nef, but is critical for CD4 down-modulation. J Gen Virol 2003;84:2705–2713.
54. Cluet D, Bertsch C, Beyer C, Gloeckler L, Erhardt M, Gut JP, Galzi JL, Aubertin AM. Detection of human immunodeficiency virus type 1 Nef and CD4 physical interaction in living human cells by using bioluminescence resonance energy transfer. J Virol 2005;79:8629–8636.
55. Thoulouze MI, Sol-Foulon N, Blanchet F, Dautry-Varsat A, Schwartz O, Alcover A. Human immunodeficiency virus type-1 infection impairs the formation of the immunological synapse. Immunity 2006;24: 547–561.
56. Singh RD, Puri V, Valiyaveettil JT, Marks DL, Bittman R, Pagano RE. Selective caveolin-1-dependent endocytosis of glycosphingolipids. Mol Biol Cell 2003;14:3254–3265.
57. Py B, Slomianny C, Auberger P, Petit PX, Benichou S. Siva-1 and an alternative splice form lacking the death domain, Siva-2, similarly induce apoptosis in T lymphocytes via a caspase-dependent mitochondrial pathway. J Immunol 2004;172:4008–4017.